International Journal of Civil Engineering

Geotechnical Engineering

Effect of multi-support excitation on seismic response of embankment dams

M. Davoodi[1,*], M. K. Jafari[2], S. M. A. Sadrolddini[3]

Received: October 2010, Revised: May 2011, Accepted: October 2011

Abstract

Spatial Variation of Earthquake Ground Motion (SVEGM) is clearly indicated in data recorded at dense seismographic arrays. The main purpose of this paper is to study the influence of SVEGM on the seismic response of large embankment dams. To this end, the Masjed Soleyman embankment dam, constructed in Iran is selected as a numerical example. The spatially varying ground motion time histories are generated using spectral representation method. According to this methodology, the generated time histories are compatible with prescribed response spectra and reflect the wave passage and loss of coherence effects. To investigate the sensitivity of the dam responses to the degree of incoherency, three different coherency models are used to simulate spatially variable seismic ground motions. Finally, the seismic response of the dam under multi-support excitation is analyzed and compared to that due to uniform ground motion. Also, the Newmark's method is used to estimate seismic-induced permanent displacements of the embankment dam. The analysis results reveal that the dam responses can be sensitive to the assumed spatial variation of ground motion along its base. As a general trend, it is concluded that the use of multi-support excitation, which is more realistic assumption, results in lower acceleration and displacement responses than those due to uniform excitation.

Keywords: Seismic response, Embankment dam, Spatial variability, Coherency loss, Wave passage.

1. Introduction

Past research studies have demonstrated that seismic ground motion can vary significantly over distances comparable to the length of the majority of large engineered structures on multiple supports. Spatial variability of seismic ground motion can be mainly attributed to the following three mechanisms: 1) difference in arrival times of seismic waves at different locations, commonly known as the "wave passage effect," 2) loss of coherence of seismic waves due to multiple reflection and refraction as they propagate through the highly inhomogeneous soil medium, referred to as the "incoherence effect," and 3) change in the amplitude and frequency content of seismic ground motion due to different local soil conditions, known as the "local soil effect" [1]. This is while the current engineering practice assumes routinely that the excitations at all support points are the same or that they differ only by a wave propagation time delay. These assumptions ignore the natural incoherence in the ground motion which may lead to incorrect or inaccurate results. SVEGM can significantly affect the seismic response of long structures such as tunnels, dams and bridges [2]. Because these structures extend over long distances parallel to the ground, their supports undergo different motions during an earthquake.

Initiated in the mid 1960s, several researchers have investigated the response of long span structures to multi-support excitations [2]. Pioneering studies analyzed the wave passage effect on the response of buildings, bridges and pipelines. Response of concrete dams to asynchronous base excitation has been studied by Calciati et al [3], Dumanoglu and Severn [4], [5]. Dumanoglu et al [6] studied the dynamic response of an embankment dam subjected to asynchronous input motion with varying traveling velocities. They concluded that with decreasing velocity of the earthquake waves, the horizontal and vertical stresses at a cross section close to the base increase appreciably. Haroun and Abdel Hafiz [7] studied the effects of amplitude and phase difference of an earthquake motion on the seismic response of long earth dams. They found that the uniform excitation produces the

* *Corresponding Author: m-davood@iiees.ac.ir*
1 Assistant professor of International Institute of Earthquake Engineering and Seismology, Tehran, I.R.Iran
2 Professor of International Institute of Earthquake Engineering and Seismology, Tehran, I.R.Iran
3 Research Assistant in International Institute of Earthquake Engineering and Seismology, Assistant professor, Department of Civil Engineering, Islamshahr Branch, Islamic Azad University, Islamshahr, I.R. Iran

maximum response for embankment dams with small length-to-height ratios, whereas the variable amplitude excitation yields the maximum response at the mid-point of the dam for relatively large length-to-height ratios. They also found that the dam response to traveling waves can be magnified considerably.

The effect of ground motion incoherence on the seismic response of structures has been studied after the installation of dense instrument arrays. Ramadan and Novak [8] investigated the axial and lateral response of long gravity dams, including dam-reservoir-foundation interaction, to spatially incoherent seismic ground motion. Their results indicated that the peak additional normal and shear stresses resulting from the ground motion spatial incoherence are quite high and should be considered together with those evaluated using conventional 2D analysis. Bilici et al. [9] analyzed stochastic dynamic responses of Sariyar concrete gravity dam subjected to SVEGM using the displacement-based fluid finite elements. They concluded that SVEGM has important effects on the stochastic dynamic responses of dam-reservoir-foundation systems.

The effect of SVEGM on seismic response of embankment dams has not been thoroughly examined in the literature. In fact, these structures have drawn the least attention among scientists, as compared to lifelines, bridges and concrete gravity dams. The first systematic studies found in the literature were made by Chen and Harichandran [10,11]. They studied the effects of SVEGM on the Santa Felicia earth dam located in Southern California. A 3-D finite element model of the dam was used for the analysis. Their results indicated that the stress response of stiff material near the base of the dam can be significantly increased due to SVEGM. They also conducted that the distribution of the maximum shear stress depended strongly on the coherency model utilized. Davoodi and Javaheri [12] studied the effect of SVEGM on the seismic response of Masjed Soleyman earth dam. They utilized a stochastic SVEGM model accounting for both incoherence and wave passage effects to specify earthquake excitation and concluded that SVEGM can have a significant effect on the stability of embankment dams.

The majority of the studies discussed above were conducted in the frequency domain using stochastic methods of analysis. Also, several response-spectrum-based procedures have been developed during the past few years with the effect of ground motion incoherency [13,14]. Both stochastic and response spectrum analysis methods cannot include the nonlinear behavior of the structure. Such a limitation makes these methods inadequate when conducting the performance-based analysis and design of significant structures such as embankment dams. In such cases, deterministic nonlinear time history analysis is necessary, with the effect of the SVEGM included in terms of multi-support excitation. This requires numerical simulation techniques to account for the spatial correlation of earthquake ground motions.

Aiming at this goal, this paper examines the seismic behavior of the Masjed-Soleyman embankment dam under spatially correlated synthetic accelerograms. A spectral-representation-based algorithm is used to generate response-spectrum-compatible time histories at different support points of the dam. In this method the ground motion time histories are generated as non-stationary stochastic vector process. The spatially varying earthquake ground motion model includes incoherence and wave-passage effects. Numerical analyses are conducted using the finite difference program (FLAC2D version 5) based on a continuum finite difference discretization using the Langrangian approach [15].

2. Site description and geotechnical characterization

2.1. Description of the dam

The Masjed Soleyman rockfill dam is constructed on Karun River in Khuzestan province in southwest of Iran, 25.5km from Masjed Soleyman city. The dam has a maximum height of 177m, width of 700m at the foundation level and crest length of 492m. It is made of a central impervious core and pervious shell upstream and downstream resting on the Bakhtiyari geological formation which is marked by hard conglomerate and very thin clay intercalation. The geometry of the maximum cross-section of the dam and its material zones are shown in Figure 1.

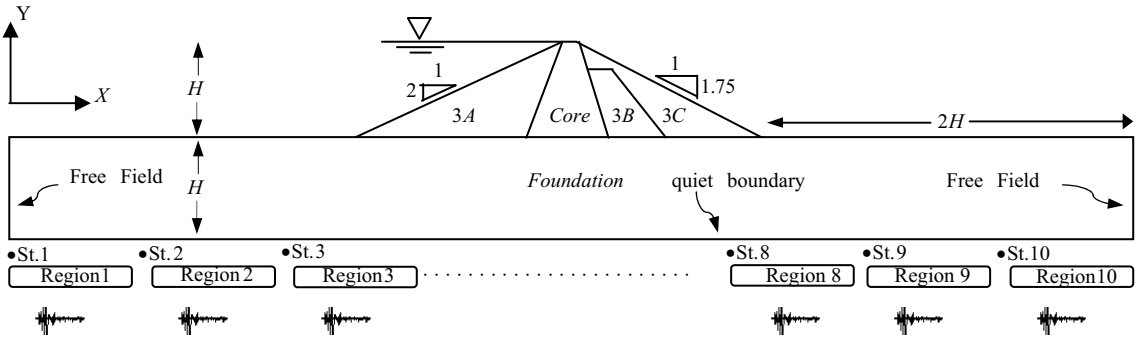

Core : Impervious clayey soils with 80% fines and 20% sand and gravel.

3A : Shell (Rockfill) - Predominately conglomerate, max particle size 1000 mm.

3B : Shell (Rockfill) - Conglomerate with sandstone and clayey siltstone, max particle size 1000 mm.

3C : Shell (Rockfill) - Conglomerate with sandstone, max particle size 1000 mm.

Foundation : conglomerate, claystone, sandstone and siltstone.

Fig. 1. Maximum cross section, material zones and illustration of multi-support excitation for Masjed Soleyman embankment dam

2.2 Material properties for numerical analysis

Reliable set of material properties for static and dynamic analyses is evaluated based on consulting engineering reports [16] and in-situ vibration tests [17, 18]. Table 1 lists the shear strength parameters as obtained from drained triaxial tests for material regions shown in Figure 1. In FLAC software, the yield criterion for problems involving plasticity is expressed in terms of effective stresses. Thus, drained values for cohesion and friction angle are assigned as material properties.

Figure 2 shows the dependency of soil stiffness on strain level for core and shell materials obtained from dynamic laboratory tests. In numerical analysis model, the Hardin/Drnevich function which is implemented as a default hysteretic damping function in Flac program is used to fit the modulus-reduction curves of the dam materials. As compared in Figure 2, this default model provides a reasonable fit to both core and shell modulus-reduction curves over the whole range of strains.

The distribution of G_0 in the dam body was estimated in the design stage based on Sawada's proposal [19] for shear wave velocity Vs distribution in the depth of rockfill dams. Also a more comprehensive attempt, aimed at establishing correct pattern of variation of small strain shear modulus with depth, has recently made by Davoodi [17] and Jafari and Davoodi [18]. They have evaluated the modified profile of small strain shear modulus in the dam body using a seismic refraction survey on the dam body, the right and the left abutments. Applying the results of latter studies, the final profile of the modified shear wave velocity used in present study is shown in Figure 3.

Table 1. Material properties of dam body and foundation materials used in numerical analysis [16]

Material		Density (ton/m^3)	Poisson ratio υ	φ (deg)	C (kPa)
Core		2.20	0.45	30.0	0.0
3A&C	Saturated	2.35	0.40	45.0	0.0
	unsaturated	2.20	0.40		
3B	unsaturated	2.2	0.40	37.0	0.0
Foundation		2.5	0.30	40.0	0.0

3. Generation of seismic accelerations

3.1. simulation algorithm

In this study, a spectral- representation-based algorithm [20] is used to generate spatially varying ground motion time histories at several locations on the ground surface. An iterative scheme is then used to match the generated acceleration time histories to target response spectrum [1]. The resulting sample functions are compatible with prescribed response spectra and reflect the wave passage and loss of coherence effects. According to applied methodology for the special case which modulating functions are independent of frequency, the elements of the cross-spectral density matrix are defined as:

$$S_{jk}^{\ 0}(\omega,t) = A_j(t)A_k(t)\sqrt{S_j(\omega)\,S_k(\omega)}\,\Gamma_{jk}(\omega)\exp[-\frac{iw\nu}{V_s}]\quad j,k = 1,2,3,4,...,M \tag{1}$$

$$S_{jj}^{\ 0}(\omega,t) = |\,A_j(t)\,|^2 S_j(\omega)\qquad j = 1,2,3,4 \tag{2}$$

Where ω is the angular frequency, M is the total number of spatial stations, j and k are the station numbers, $S_{jj}(\omega)$ are auto spectral density functions, $S_{jk}(\omega)$ are cross spectrum of the motions between the two stations j and k, $A_j(t)$ are modulating functions, $\Gamma_{jk}(\omega)$ are the coherence functions between the ground motions generated at stations j and k, ν is separation distance and V_s is velocity of shear wave propagation. Both incoherence and wave passage effect are considered in equation 1 to specify the base motions in the upstream-downstream direction. By using spectral-representation

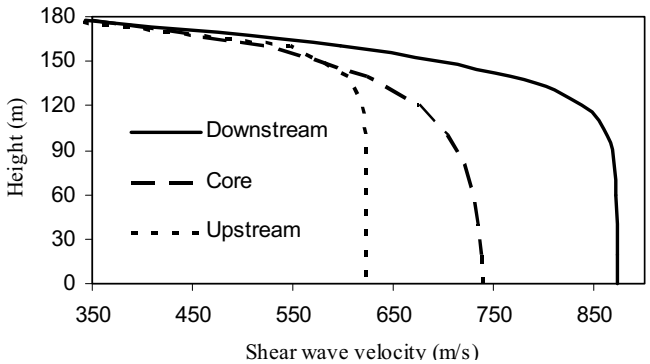

Fig. 3. Profile of shear wave velocity in the dam body (m/s) [18]

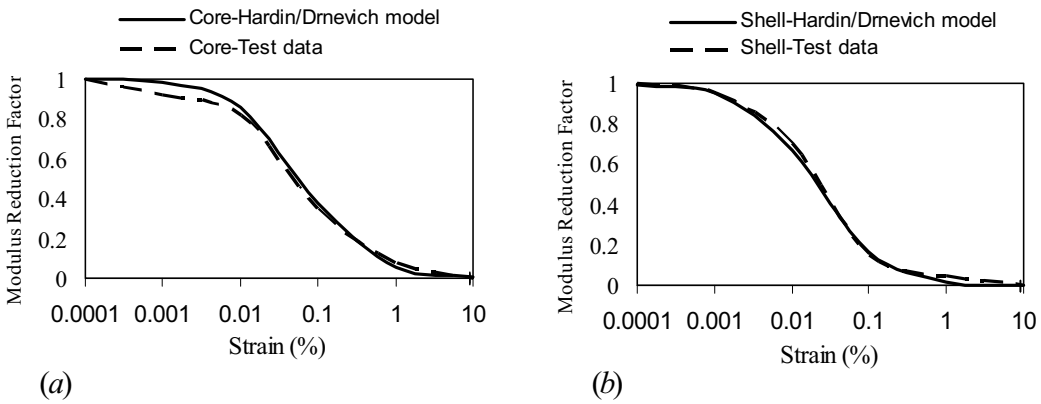

Fig. 2. Variation of shear modulus with strain (a) for core material (b) for shell materials

method, stationary stochastic vector process $f_j(t)$; j=1,2,3,…M can be simulated by the following series:

$$f_j(t) = 2\sum_{m=1}^{j}\sum_{l=1}^{N} | H_{jm}(\omega_l, t) | \sqrt{\Delta\omega} \cos[\omega_l t - \theta_{jm}(\omega_l, t) + \phi_{ml}]$$

$$j = 1,2,3,..., M \tag{3}$$

Where:

$$\omega_l = l\,\Delta\omega \qquad l = 1,2,..., N \tag{4}$$

$$\Delta\omega = \frac{\omega_u}{N} \tag{5}$$

$$\theta_{jk}(\omega) = \tan^{-1}\left[\frac{\mathrm{Im}[H_{jk}(\omega)]}{\mathrm{Re}[H_{jk}(\omega)]}\right] \tag{6}$$

In Eq. (3) to (6), $H(\omega,t)$ is a lower triangular matrix obtained by cholesky decomposition of cross spectra density matrix at every time instant t ,φ_{ml} are sequences of random phase angles uniformly distributed over the range [0,2 π], ω_u represents an upper cut-off frequency, N is the total number of frequency samples, and Im[$H_{jk}(\omega,t)$] and Re[$H_{jk}(\omega,t)$] are the imaginary and real parts of the $H(\omega,t)$ respectively. It is important to emphasize that the non-uniform acceleration time histories at ground surface are generated compatible with the three prescribed target quantities: (1) target response spectra, (2) complex coherency functions, and (3) modulating functions. In the following section three abovementioned quantities will be outlined.

3.2. Target quantities

Studies by Harichandran and Vanmarcke [21] showed that local variation in the power spectrum of the ground motion could be neglected within areas of uniform soil conditions and geology. In this study, it is assumed that this condition exists within the base dimensions of embankment dams. Therefore, the spatially variable ground motion time histories are generated to match a unit target response spectra obtained from seismic hazard analysis results [17]. The normalized target acceleration response spectrum is shown in Figure 4. Considering the effects of all active faults located in the earth dam site, peak horizontal ground acceleration for Maximum Credible Level (MCL) is set equal to 0.45g.

To investigate the sensitivity of the dam responses to coherency models, spatially variable ground motions are generated based on three widely used coherency models. The first model proposed by Harichandran-Vanmarcke [21] is based on the study of four events recorded by the SMART-1 array in Taiwan. This model has the form:

$$|\gamma(\upsilon, f)| = A\exp\left[-\frac{2\upsilon}{\alpha\theta(f)}(1 - A + \alpha A)\right] + (1 - A)\exp\left[-\frac{2\upsilon}{\theta(f)}(1 - A + \alpha A)\right] \tag{8a}$$

where

$$\theta(f) = k\left[1 + (f/f_0)^b\right]^{-1/2} \tag{8b}$$

In which A, α, κ, f_o and b are the model parameters, υ is separation distance between two stations and f is frequency in Hertz. The model parameters were estimated by Harichandran and Wang [22] as, A=0.626; α = 0.022; k = 19700; f_0 = 2.019 and b=3.47. As for other multiple-parameters models, this model can be made to match a broad range of coherency applications.

The second coherency model considered is that proposed by Abrahamson [23] which is based on a number of earthquake events in California and Twain. This model has the advantage that it can be used for a broad range of soil conditions and has the form:

$$|\gamma_1(f, \upsilon)| = \tanh\left[\frac{C_3(\upsilon)}{1 + C_4(\upsilon) f + C_7(\upsilon) f^2} + (4.8 - C_3(\upsilon))\exp(C_6(\upsilon) f) + 0.35\right] \tag{9}$$

$$C_3(\upsilon) = \frac{3.95}{(1 + 0.0077\upsilon + 0.000023\upsilon^2)} + 0.85\exp(-0.00013\upsilon) \tag{10}$$

$$C_4(\upsilon) = \frac{0.4\left[1 - \frac{1}{1 + (\upsilon/5)^3}\right]}{\left[1 + (\upsilon/190)^8\right]\left[1 + (\upsilon/180)^3\right]} \tag{11}$$

$$C_6(\upsilon) = 3(\exp(-\upsilon/20) - 1 - 0.0018\upsilon \tag{12}$$

$$C_7(\upsilon) = -0.598 + 0.106\ln(\upsilon + 325) - 0.0151\exp(-0.6\upsilon) \tag{13}$$

In which υ is separation distance and f is frequency in Hertz.

The third coherency model considered is that proposed by Hindy and Novak [24] as a simple coherency model. Their model was employed successfully in other random fields, such as wind and offshore engineering. In this model, the coherency variations with separation, v, and frequency, f, are combined in a single dimensionless frequency in the form:

$$|\gamma(\nu, \omega)| = \exp\{-\alpha(2\pi f \nu)^\beta\} \tag{14}$$

The model parameters used as, α = 0.07780; β = 0.31.

The value of the coherency decays with the frequency and station separation distance. Figure 5 compares the decay with frequency of the three coherency models at separation distance of 290 m. This distance is corresponding to the location of the station No. 2 as shown in Figure 1. It can be seen that in comparison to the other models, the Abrahamson model produces

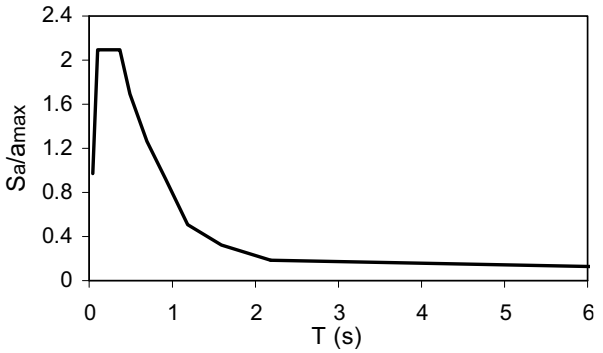

Fig. 4. Normalized target response spectra for ground motion generation [17]

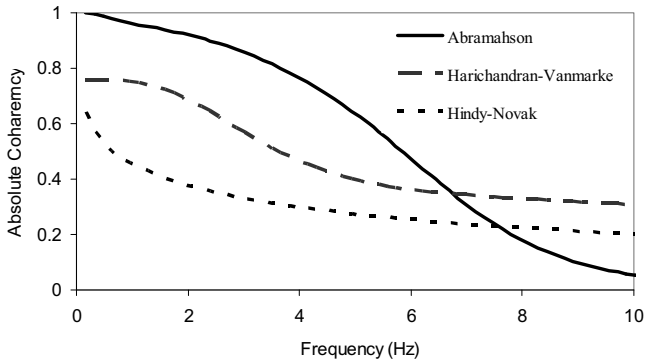

Fig. 5. Coherency decay for three considered models (υ=290m)

smaller coherency loss especially at low frequency ranges.

As a third target quantity the Jennings [25] envelope function used for the modulation purpose:

$$A(t)=\begin{cases}\left(\dfrac{t}{t_0}\right)^2 & 0\le t\le 2\\ 1 & 2\le t\le 9\\ e^{-0.4(t-t_a)} & t\ge 9\end{cases} \quad (15)$$

4. Application

4.1. Dynamic loading cases

The seismic behavior of Masjed Soleyman dam is investigated under a total of five different loading cases, representing different kinds of variations in the base excitations. Table 2 describes the five loading cases in more detail considering the characteristics of dynamic excitation. The continuous contact between the foundation and the half space is represented by a finite numbers of support points. Since this number of multi support excitation is too large for dam type structures, so the base of the dam is divided into ten regions and the generated motions are applied at each one. The configuration of the stations and the base dynamic loading regions is shown in figure 1. It is assumed that all support points located within a region have identical excitation.

4.2. Generated time histories

The simulation is performed at 6144 time instants, with a time step Δt = 0.00307 sec, over a duration equal to 18.86 sec [1]. The upper cut-off frequency ω_u and the value of N are set equal to 128 rad/sec and 128 respectively. It is worth mentioning that the generated records are firstly assumed to be provided as outcrop motions, applied to a rock outcropping located at the base of the dam (motion (a) in Figure 6). Motion (b) at the bottom of the dam foundation is obtained by deconvolution of the outcropping target accelerogram to the assumed foundation depth. Deconvolution analysis is studied using the code SHAKE91[26].

The acceleration time histories generated at the station No. 3 for different cases are shown for instance in Figure 7. Space limitations preclude the presentation of all of the generated motions. In Figure 8 the pseudo acceleration response spectra for the records generated at the station No. 3 are compared with the target one. It can be inferred that the generated time histories are in a good agreement with the target response spectrum. Due to the same frequency content and close intensities, the only difference between the motions of different stations can be attributed to the incoherency and wave passage effect.

5. Numerical model

The mid-section of the dam is modeled as a 2D finite difference grid. To avoid numerical distortion of the propagating wave during the dynamic analysis, the maximum height of elements of the dam is smaller than 1/5 of the wavelength λ_{min} associated with the highest frequency

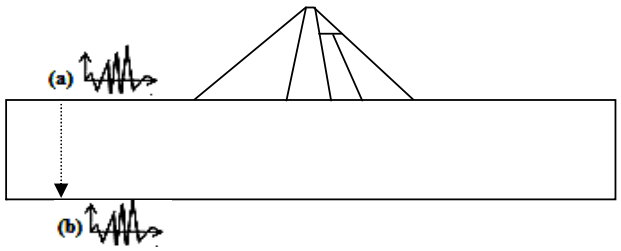

Fig. 6. Scheme of deconvolution analysis for evaluating the foundation input motion

Table 2. Detailed description of different loading cases

Loading case name	Type of generated ground motion	Spatial variability effects considered	Coherency function	Velocity of wave propagation
Case 1	Incoherent	Only the incoherence effect considered	Abrahamson	–
Case 2	Incoherent	Only the incoherence effect considered	Harichandran and Vanmarcke	–
Case 3	Incoherent	Only the incoherence effect considered	Hindy and Novak	–
Case 4	General	Both the wave passage and incoherence effects considered	Harichandran and Vanmarcke	1200 m/s
Case 5	uniform	–	–	–

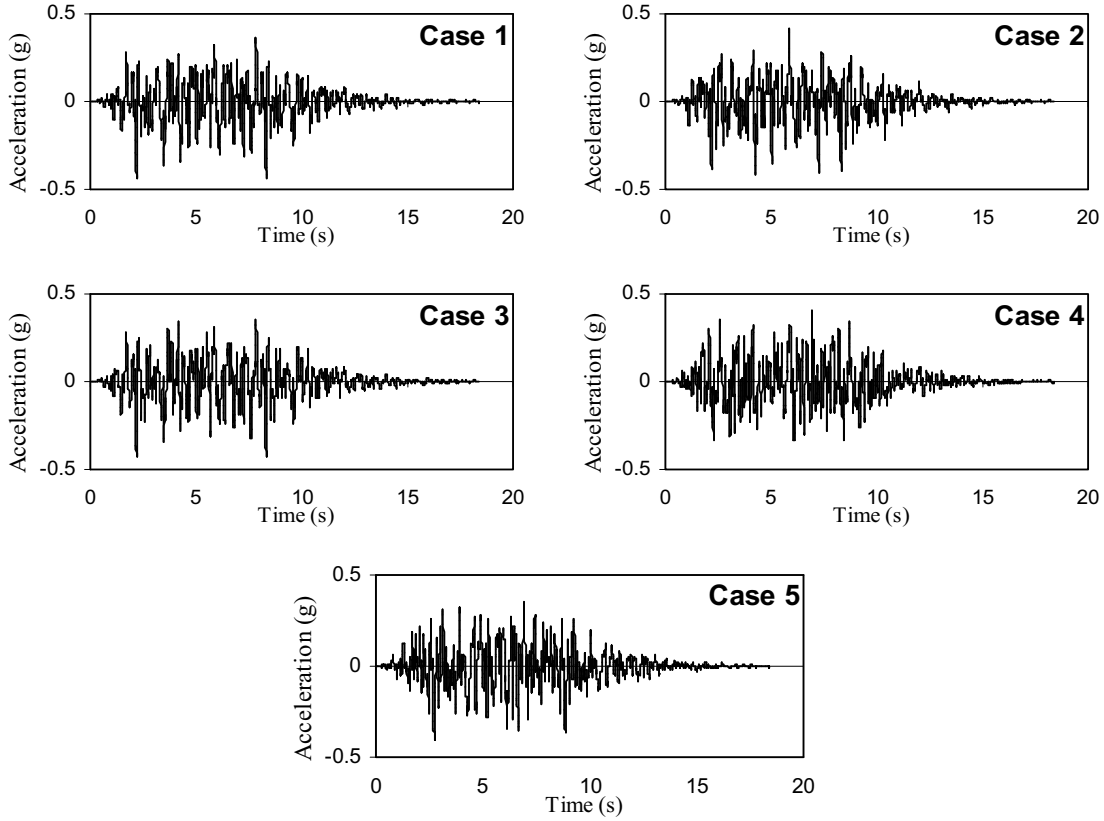

Fig. 7. Generated acceleration time histories at station No.3 for different loading cases

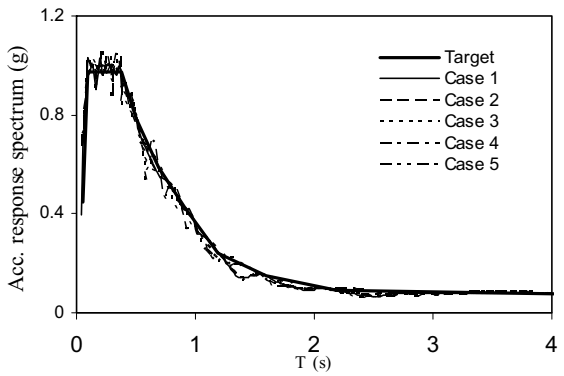

Fig. 8. Response spectrum comparison of generated records with the target one at station No.3 for different loading cases

component of the input wave f_{max} [27]. The largest zone size in the numerical model (Δl) is selected as 7.5 m. Thus, the maximum frequency (f_{max}) that can be modeled accurately is 9.33 Hz. The input motions were then low pass filtered removing frequency components higher than 8 Hz. This filtering value is selected to account for the reduction in shear wave velocity that may occur in some of the materials during the strong motion loading stage.

The finite difference analyses are carried out adopting hysteretic damping and elastic-perfectly plastic Mohr-Coulomb material behavior. The accurate numerical analysis of the seismic response of the dam body requires the modeling of the real flexible material of the foundation. The depth and lateral extent of the foundation are shown in Figure 1. The boundary conditions along the vertical and horizontal edges of the Finite difference model are illustrated in Figure 1 too. The boundary conditions at the sides of the model must account for the free-field motion which would exist in the absence of the structure [28]. The absorbent boundaries are based on the scheme described by Lysmer and Kuhlemeyer [29] in which an increase in stress on the boundary is absorbed independently of the frequency of the incident waves.

6. SVEGM effect on the seismic response of the dam

This section compares the seismic responses of the Masjed Soleyman earth dam under uniform and multi-support excitations. The analysis results in this section will be presented in terms of acceleration and displacement fields for different loading cases introduced in section 4.1.

6.1. Acceleration field

Figure 9 compares the variation of acceleration response with depth along the centre line of the dam cross section, as obtained by applying uniform and multi-support excitations. Comparisons are in terms of the peak and Root Mean Square (RMS) of the computed acceleration time histories. Three important points can be concluded from this figure. First, at all elevations the acceleration responses due to multi-support excitations are sensitive to the coherency model used in simulation process. Second, the use of identical ground motion in such a tall dam, generally overestimates the acceleration responses of the dam. Specifically, compared to multi-support

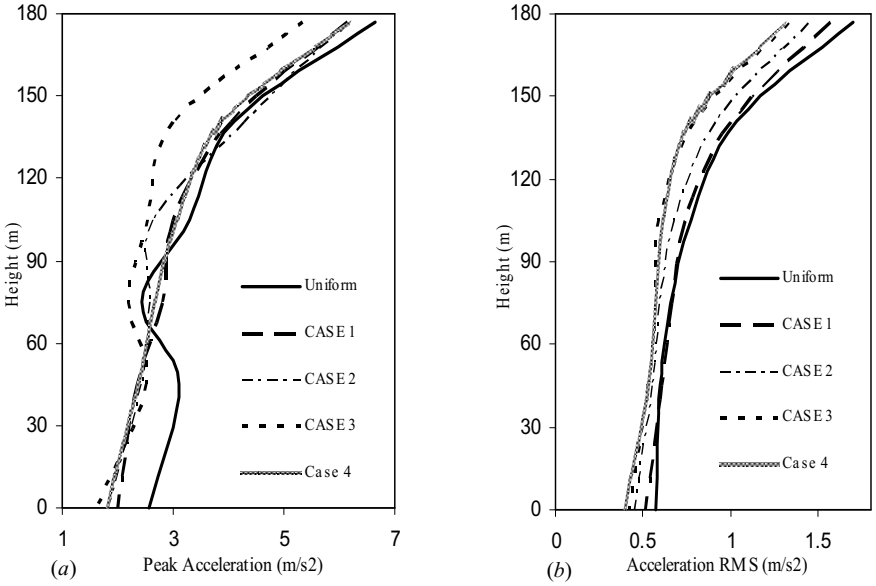

Fig. 9. The variation of (a) peak accelerations and (b) RMS of the acceleration responses with depth for uniform and multi-support excitations

excitations, the uniform excitation results in a 8 to 20 percent increase in crest peak acceleration. In the lower parts of the dam, in spite of some scattering, the peak and intensity of accelerations due to multi-support excitations don't exceed than those due to uniform excitations. Third, Comparison of the acceleration RMS for loading cases 2 and 4 reveals that the wave passage effect decreases considerably the acceleration responses at all elevations.

Considering Figure 9 the effect of the degree of incoherency on the acceleration responses can be explored too. As can be seen, at all elevations, applying the loading cases 2 and 3 yields the lower acceleration RMS values than those due to loading case 1. A hint at the cause of such a discrepancy may be provided by considering the lowest degree of incoherency provided by Abrahamson model over a broad frequency ranges. Thus, it may be mentioned that the higher the degree of incoherency, the lower the intensities of acceleration responses within the core of the dam.

To investigate the effect of SVEGM on the frequency content of the acceleration response, the Fourier amplitude spectrums FA of the crest accelerations are compared in Figure 10. Three conclusions may be drawn from this figure. (i) It is apparent that the frequency responses are mainly sensitive to the coherency models. (ii) As a clear trend, in the lower frequency range (0.0 Hz to 2 Hz) applying Hindy and Novak coherency model with higher coherency decay, produces the least peaks compare to those of identical ground motion. Whereas the peaks of two other models with lower coherency decays are

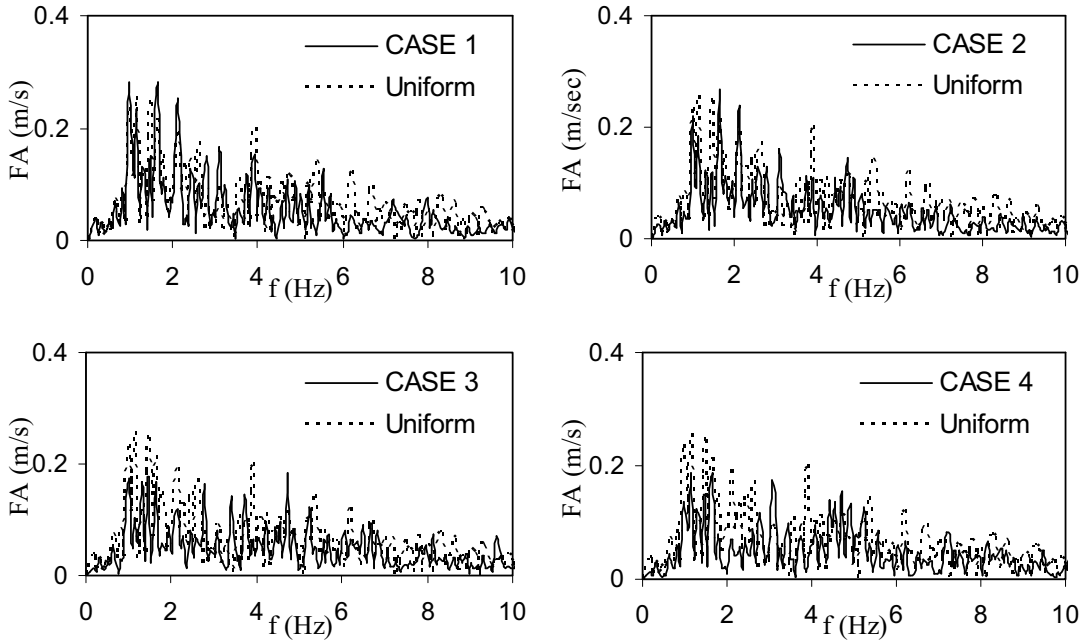

Fig. 10. Comparison of the Fourier spectra density functions of crest accelerations for uniform and multi-support excitations

close to those of identical ground motion. (iii) Comparison of the results for loading cases 2 and 4 indicates that in unison with the third result discussed above, the wave passage effect decreases the Fourier amplitude of crest acceleration response.

6.2. Displacement field

Figure 11 compares the settlement profiles at the core axis computed at the end of the dynamic analysis under uniform and multi-support excitations. Very small displacements are observed in the lower two-thirds of the dam for both uniform and non-uniform excitations. This kind of behavior is also observed by other researchers for displacement response of embankment dams [30,31]. The latter can be explained by considering the specific geometrical properties of the embankment dams which cause increased displacement levels near the top of the dam. Moreover, from Figure 3 it can be inferred that at the height less than 120m, the shear wave velocities are considerably higher than those in the upper elevations of the dam. Thus, the resultant settlements of stiff materials located at the height less than 120m are very small. Consequently, due to very small displacements observed in the lower part of the dam, the response differences between uniform and multi-support excitations do not take place considerably at lower parts of the dam.

As can be seen form figure 11, in the upper elevations, the settlements due to uniform excitations are larger than those under multi-support excitations. In other words, the incoherent accelerograms decrease the settlement response of the dam within the core. It is also clear that the displacement responses of the dam are sensitive to the coherency model.

As Figure11 indicates, the settlements due to the loading cases 1 and 2 are closer to those obtained by uniform excitations. While applying the loading cases 3 and 4 yields smaller settlements than those of uniform excitation. It is safe to express from this figure that the non uniform input motions with the high degree of incoherency produce the lower permanent displacements. Also, it is evidenced that, the wave passage effect reduces considerably the crest settlement.

Figure 12 compares the horizontal displacement time histories computed at the crest under uniform and multi-support excitations. The same trend discussed above is valid for horizontal displacements. As can be seen in this figure, the maximum displacement produced by uniform excitation is larger than that of non-uniform excitations. The displacement response trends observed in this study are in general agreement with the Chen and Harichandran [10] results in the sense that the displacements and strains obtained by uniform excitations are slightly conservative within the core and are acceptable.

6.3. Permanent displacements of slip surface

In 1965, Newmark [32] proposed use of an analogy to sliding block on an inclined plane. In this approach, a dam body is modeled as a rigid block with a thin failure surface along which plastic slip may occur in one direction. The procedure is illustrated in Fig. 13. If the acceleration pattern acting on the potential sliding mass is similar to that shown in the figure, then no displacement will occur until time t1, when the induced acceleration reaches the yield acceleration for the first cycle k_{y1}. Between times t1 and t2, the velocity of the sliding wedge will increase. The velocity will gradually decrease and become equal to zero at $t = t_3$. The displacement of the soil wedge can now be determined by integration of the area under the velocity versus time plot between t_1 and t_3. For the prediction of permanent displacement of sliding blocks on the dam, the Makdisi and Seed [33] simplified method was used for selected potential surface. This simplified method includes two steps:

1. Perform a dynamic analysis of the dam assuming that the

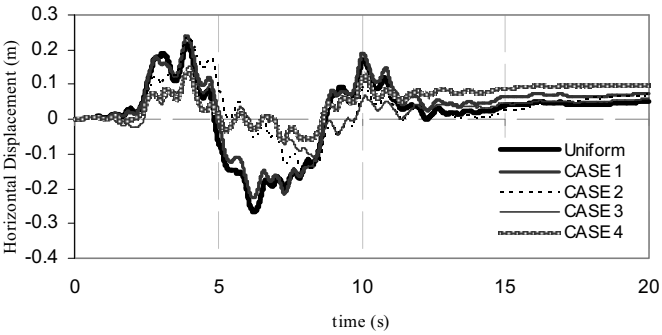

Fig. 12. Crest horizontal displacement time histories computed under uniform and multi-support excitations

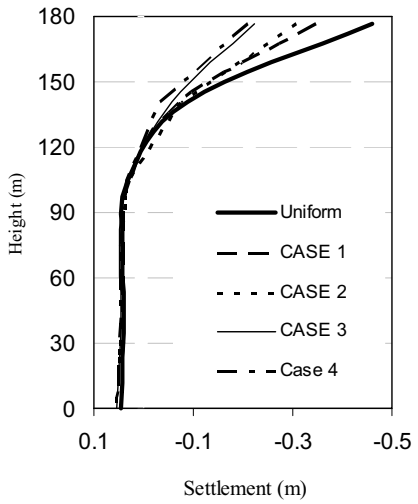

Fig. 11. Vertical permanent displacement profile computed along the dam centre line for uniform and multi-support excitations

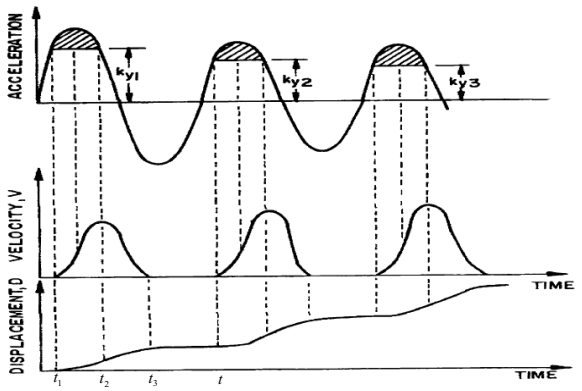

Fig. 13. Integration procedure of accelerograms to determine down-slope permanent displacements

failure surface does not exist. Determine the time history of an average acceleration for the soil above the failure surface.

2. Use this average time history of acceleration as input to a sliding block analysis and compute the resulting permanent slip along failure surface.

Combining two abovementioned steps and computing the seismic deformation at the dam is termed the decouple model [34]. Figure 14 shows the adopted sliding surface for the upstream side of the dam [17]. A pseudo-static analysis by using SLOPE/W software [35] is performed in order to determine the corresponding yield acceleration. The material properties used in pseudo-static analysis are given in Table 1. The critical seismic coefficient (*ky*) is evaluated equal to 0.29g for the selected sliding surface. This means that if the average acceleration along the slip surface overtakes the critical value of 0.29g, the sliding mass will start moving as a rigid block.

In this study, a computer programs is written to calculate the permanent displacement of sliding mass by the method discussed above. The maximum values of averaged acceleration time history a_{max} are listed in table 3 for different loading cases. As can be inferred, the a_{max} is lower than the computed critical acceleration for the loading cases 3 and 4. Consequently, the Newark method does not predict any permanent displacement within the dam for these loading cases. Permanent displacement analysis results for uniform and other non-uniform loading cases are presented in Figure 15. As can be seen, the permanent displacements evaluated under incoherent excitations are smaller than those due to uniform excitation. In other words, the uniform excitation conservatively results in larger permanent displacements.

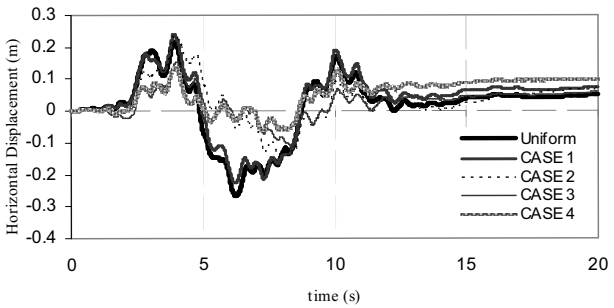

Fig. 14. The selected slip surface for the upstream side of the embankment dam [17].

Table 3. Maximum value of the average time history of acceleration computed over the volume of sliding wedge

Loading case name	Case 1	Case 2	Case 3	Case 4	Case 5
a_{max} (g)	0. 56	0.412	0.276	0.27	0.58
K_y (g)			0.29		

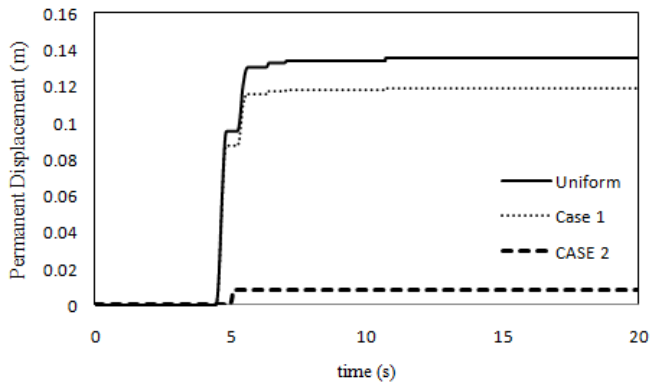

Fig. 15. Permanent displacement time histories of the sliding mass obtained for uniform multi-support excitations

7. Summary and conclusions

The seismic response of Masjed Soleyman rockfill dam under multi-support excitation was computed using the finite difference program FLAC2D. The numerical study results reveal that the dam responses can be sensitive to the assumed spatial variation of ground motion along its base. As a general trend, it is observed that applying the incoherent ground motions yields the lower acceleration and displacement responses than those due to uniform excitation.

The sensitivity of dynamic responses of the dam to the degree of incoherency was investigated too. It is generally concluded that, higher coherency decay yields lower acceleration and displacement responses of the dam. This indicates that the dam responses under uniform excitation will be more conservative to design.

It is found that in unison with the general trend, the incoherent excitations result in very small permanent displacements. The observations are in general agreement with the Chen and Harichandran [10] results which studied the effects of SVEGM on the Santa Felicia earth dam. It is concluded that more reduction in acceleration and displacement responses of the dam can be observed if the wave passage effect is also modeled in ground motion generation.

Acknowledgements: This paper is a part of the research project with the title of "Effect of spatial variation of Earthquake Ground Motion on Dynamic Behaviour of Embankment Dams" funded by the International Institute of Earthquake Engineering and Seismology (IIEES) under activity code of 6128 and project code of 450. This support is gratefully acknowledged

References

[1] Shinozuka M., Saxena V. Deodatis G.:2000, Effect of Spatial Variation of Ground Motion on Highway Structures. MCEER-00-0013.

[2] Zerva A, Zervas V.: 2002, Spatial variation of seismic ground motions: an overview, Applied Mechanics Review, ASME, Vol. 55 (3): 271-297.

[3] Calciati, F. et al: 1979, Experiences Gained During In-Situ Artificial and Natural Dynamic Excitation of Large Concrete Dams in Italy, Int. Congress on Large Dams (ICOLD), New Delhi, References 4, R32.

[4] Dumanoglu, A.A. and Severn, R.T.:1982, Multiple-Support Base Excitation of Structures, Proceedings 7th European Conference on Earthquake Engineering, Athens

[5] Dumanoglu, A.A. and Severn, R. T.: 1984, Dynamic Response of Dams and Other Structures to Differential Ground Motions,

Proc. Inst. Civ.Engrs., Part 2,77, 333-352
[6] Dumanoglu A.A., Severn, R.T., and Taylor, C.A.: 1984, Effect of Asynchronous Input on the Response of Dams, Proceedings of 8th World Conference on Earthquake Engineering, 6(127), SanFrancisco.
[7] Haroun, M.A. and Abdel-Hafiz, E.A.: 1987,Seismic Response Analysis of Earth Dams Under Differential Ground Motion , Bul. Seism. Soc.Am., 77(5), 1514-1529.
[8] Ramadan O. and Novak M.: 1993, Response of long gravity dams to incoherent seismic ground motions, Transactions on the Built Environment, Vol 3, WIT Press, ISSN 1743-3509
[9] Bilici, Y., Bayraktar, A., Soyluk, K., Haciefendioglu, K., Ates, S. and Adanur, S.: 2009, Stochastic Dynamic Response of Dam-Reservoir-Foundation Systems to Spatially Varying Earthquake Ground Motions, Soil dynamics and Earthquake Engineering, 29: 444-458.
[10] Chen MT, Harichandran RS.: 2001, Response of an earth dam to spatially varying earthquake ground motion, Journal of Engineering Mechanics, 127(9):932–9.
[11] Chen M. and Harichandran R. S.: 1998, Sensitivity of earth dam seismic response to ground motion coherency, Geotechnical Earthquake Engineering of Soil Dynamics, vol.2, N75, 914-925
[12] M. Davoodi and Javaheri A.: 2008, Evaluating the Stability of Masjed Soleiman Dam Sliding Surfaces in Uniform and SVEGM Excitations Journal of Seismology and Earthquake Engineering 9(4), (in Persian)
[13] Berrah MK, Kausel E.: 1992, Response spectrum analysis of structures subjected to spatially varying motions, Earthquake Engineering and Structural Dynamics, 21:461–70.
[14] Der Kiureghian A, Neuenhofer A.: 1992, Response spectrum method for the multi-support seismic excitation, Earthquake Engineering and Structural Dynamics, 21:713–40.
[15] Itasca Consulting Group. FLAC, 2005, Fast Lagrangian Analysis of Continua, Version 5.0, Itasca Consulting Group, Minneapolis, Minnesota
[16] Nippon Koei, Moshanir, Lahmeyer: 1999, Masjed-E-Soleiman HEEP Report on Dynamic Analysis for the Masjed-E-Soleiman Dam
[17] Davoodi, M.: 2003, Dynamic characteristic evaluation of embankment dams by forced and ambient vibration tests Ph.D. Thesis, International Earthquake Engineering and Seismology (IIEES), Tehran, I.R. Iran, (in Persian)
[18] Jafari, M.K. and Davoodi, M.: 2006, Dynamic Characteristics Evaluation of Masjed Soleiman Dam Using In-situ Dynamic Tests, Canadian Geotechnical Journal, 43(10), 997~1014
[19] Sawada, Y. and Takahashi, T.: 1975, Study on the material properties and the earthquake behaviors of rockfill dam, Proc. of 4th Japan Earthquake Engineering Symposium, pp.695-702, 1975.
[20] Deodatis G.: 1996, Non-stationary stochastic vector processes: seismic ground motion applications, Probab. Eng. Mech. 11, 149–168.
[21] Harichandran RS. And Vanmarcke E.H.: 1986, Stochastic variation of earthquake ground motion in space and time, Journal of Engineering Mechanics, 112:154–74
[22] Harichandran, R. S. and Wang, W.: 1990, Effect of Spatially Varying Seismic Excitation on Surface Lifelines, Proceedings of Fourth U.S. National Conference on Earthquake Engineering, Vol. 1, pp. 885~894
[23] Abrahamson, N. A.: 1993, Spatial variation of multiple support inputs. Proceedings, 1st U. S. Seminar on Seismic Evaluation and Retrofit of Steel Bridges, Department of Civil Engineering and California Department of Transportation, University of California at Berkeley, San Francisco, California
[24] Hindy A, Novak M.: 1980, Pipeline response to random ground motions, Journal of Engineering Mechanics, 106:339–60.
[25] Jennings PC. Housner GW, Tsai NC.: 1968, Simulated earthquake motions, Techinal report, Earthquake Eng. Research Laboratory, California Institute of Technology, Pasadena,CA,
[26] Idriss IM, Sun JI. A.: 1992, Computer program for conducting equivalent linear seismic response analyses of horizontally layered soil deposits. Davis: Center for Geotechnical Modeling, Department of Civil and Environmental Engineering, University of California
[27] Kuhlemeyer RL, Lysmer J.: 1973, Finite element method accuracy for wave propagation problems. J Soil Mech Found. 99(5):421–7.
[28] Itasca Consulting Group, Inc: FLAC: 2006, Fast Lagrangian Analysis of Continua, Ver. 5.0 User's Manual, Itasca, Minneapolis,
[29] Lysmer J, Kuhlemeyer RL.: 1996, Finite dynamic model for infinite media, J Eng Mech ASCE; 95(4):859–77.
[30] Ohmachi T, Kuwano J.:1994, Dynamic safety of earth and rock fill dams. Rotterdam: A.A. Balkema.
[31] Özkan M, Özyazicioglu M, Aksar U D.:2006, An evaluation of Güldürcek dam response during 6 June 2000 Orta earthquake. Soil Dynamics and Earthquake Engineering, 26(5): 405–419.
[32] Newmark, N. M.: 1965, Effects of earthquakes on Dams and Embankments. Geotechnique, 15, 140-158.
[33] Makdisi, FI. And Seed H.B.: 1987, Simplified Procedure For Estimating Dam And Embankment Earthquake-Induced Deformation, Journal of Geotechnical Engineering, ASCE, Vol. 104, NO.GT7, P :849-867
[34] Lin JS, Whitman RV.: 1983, Decoupling approximation to the evaluation of earthquake-induced plastic slip in earth dams, Earthq Engng Struct Dyn;11:667–78.
[35] GEO-SLOPE OFFICE,: 2003, SLOPE/W for slope stability analysis (version 5)